Neutron scattering from Os isotopes at 60 keV and Re-Os nucleochronology

R. L. Hershberger, R. L. Macklin,* M. Balakrishnan, N. W. Hill,* and M. T. McEllistrem
Department of Physics and Astronomy, University of Kentucky, Lexington, Kentucky 40506
(Received 9 May 1983)

Neutron elastic and inelastic scattering cross sections have been measured for 60.5 keV neutrons incident on ^{187,188}Os. For ^{187}Os the cross section for elastic scattering is 11 b and for inelastic scattering to the 9.75-keV level it is 1.13 b. These results and other scattering properties are represented in phase shift and scattering potential analyses, which then allow the prediction of neutron capture by ^{187}Os nuclei in the 9.75-keV and ground levels. Capture rates thus provided are used in the Re-Os nucleochronology, and lead to a long galactic age, about 18 to 20 Gyr.

[NUCLEAR REACTIONS ^{187,188}Os(n,n) and ^{187}Os(n,n'), $E_n=60.5$ keV; measured $\sigma(\theta)$; phase shift and potential analyses; deduced galactic age of 18 to 20 Gyr.]

INTRODUCTION

This paper reports measurements and analyses of neutron scattering cross sections for 60.5 ± 0.5 keV neutrons scattered from ^{187,188}Os. These scattering cross sections together with other low energy scattering properties are important for two types of studies. The first deals with the surprisingly large effects of collective nuclear excitations on low energy neutron scattering.[1] The second deals with the duration (Δ) of nucleosynthesis of elements formed in *r*-process and *s*-process neutron capture, as determined from the Re-Os nucleochronology.[2] Only the second subject is of concern here.

The age of the universe (A_u) is often treated as composed of three periods, one of initial condensation into galaxies of about 1 to 2 Gyr (δ), a second of element nucleosynthesis occurring in stars and supernovae (Δ), and finally the period following the condensation of our own solar system (A_e) from the debris of earlier stars. Thus the age is given as $A_u=\delta+\Delta+A_e$, expressed in Gyr. The isotope abundance ratios of heavy elements, which have been synthesized through successive neutron captures and subsequent decay processes, provide clues from which Δ can be fixed. The age of the earth A_e, is quite well known,[3] so determination of Δ would lead to A_u.

Two nucleochronologies have been developed to the point that they could be expected to provide reliable estimates of Δ. One of these relies upon the abundance ratios of the U and Th isotopes, and their formation processes in supernovae. Since both U and Th are formed under the same explosive conditions in rapid, sequential neutron captures (*r* process) followed by β decays and, for some elements, spontaneous fission decays, they have similar histories. Thus their relative abundances are not very dependent upon the history of supernovae. The U-Th chronology had been developed by Fowler and Hoyle[4] and then had been refined by Fowler[5] to yield a Δ of 6.1 ± 2.3 Gyr. When this Δ was combined with the known[5] age of the earth, 4.6 Gyr, and an anticipated 1—2 Gyr period prior to the onset of nucleosynthesis, one had a universe age A_u of 12 ± 3 Gyr. This age corresponded well to that implied by Twarog's age-metallicity relationship for old stars[6]; that implied $A_u=13\pm3$ Gyr. This relatively young age was also supported in Tinsley's star formation model.[7] Other astrophysics studies, however, cited in the final reference of this paper, support the idea of a much older universe; that subject will be discussed in a separate communication dealing with ages implied from this study.

Another chronology for determining Δ and therefore A_u follows from the suggestion of Clayton[8] that Os isotope abundance ratios should provide an excellent test of the period of nucleosynthesis. The nuclide ^{187}Os is synthesized in part by the β decay of ^{187}Re, whose half-life $t=45.5$ Gyr (Ref. 9) is especially appropriate for timing multigigayear intervals. Both ^{187,188}Os are also formed and depleted by sequential neutron capture in stars (*s* process). For most nuclei the *s*-process contributions are well defined by measured neutron capture rates, following the many studies of Macklin and collaborators.[10] Thus, if neutron capture cross sections for the Os isotopes are carefully measured, and averaged for a stellar interior temperature such as a kT of 30 keV, the relative abundances of ^{186}Os, ^{187}Os, and ^{188}Os associated with the *s* process can be well determined. The ^{187}Os in excess of that expected from the *s* process, then, is from ^{187}Re decay, which fixes Δ.

Measured capture cross sections for Os isotopes[11,12] show similar neutron energy dependencies, and the Re-Os chronology depends only on abundance ratios. Thus the results are, fortunately, not very sensitive to the assumed stellar temperature, often taken to be near 30 keV.[8,12] Determining fractions of the ^{187}Os abundance formed through the *s* process and through ^{187}Re decay is precisely the program pursued by groups at two laboratories for some years.[2,11,12] Browne and Berman at Livermore[2,11] and Winters *et al.*[12] at ORELA have carefully measured and rechecked the capture rates so that the most recent results from the two centers are in good agreement. These authors also provide an excellent overview of the Re-Os chronology, and Browne and Berman in addition discuss

parameters important to the chronology other than the capture rates, showing that most of them are well defined.[11] The two recent studies, Refs. 11 and 12, find Δ to be 10.4 and 10.8 Gyr, respectively. This discordance with U-Th chronology and other universe dating methods was serious enough to cause concern among astrophysicists developing models of star formation.[7]

There are two potential problems with the Re-Os method and thus the dates cited above. One is that ^{187}Re itself continues to be formed through the r process. To understand the ^{187}Re β-decay rate one must know the history of the formation rate, or the history of supernovae, the sources of the intense neutron fluxes of the r process. Conventional r-process models suggest that the frequency of supernovae decays exponentially with time, with a decay constant d_R. Some models[13] had led to the conclusion that $d_R \sim (0.43\Delta)^{-1}$, and this was the value used in the most recent Re-Os chronology papers.[11,12] Fowler pointed out in 1978 that this r-process history is not a good choice[5,14]—it leads to problems with the ^{26}Al-^{26}Mg ratios detected in meteorites. The preferred value now is $d_R\Delta \sim 1.1$ which leads[5] to an age of the earth

$$A_e = 4.4 \pm 0.3 \text{ Gyr} ,$$

in good agreement with the currently accepted[3] value of 4.6 Gyr. This change in d_R would actually increase the average of the recent results of Refs. 11 and 12 from 10.5 to 12.5 Gyr. Thus updating d_R makes the discrepancy between Re-Os and U-Th dating worse, and a clear conflict.

There is another problem with, and possible source of change in, results of the Re-Os method, as pointed out by Fowler in 1972.[15] Estimating s-process produced abundances of the Os isotopes is based on laboratory capture cross sections,[11,12] and a correction must be made for the fact that in stars with an average temperature of 30 keV, capture can also occur from the 9.75-keV excited level of ^{187}Os. This correction is made using conventional models[11,12] to estimate its size. But the possibility that that correction is substantially different than calculated has currently been regarded as the expected[16] source of reconciliation between the two chronologies.

The ^{187}Os nuclei have 48% occupancy of the $\frac{3}{2}^-$ excited level at stellar temperatures,[16] and only 33% for the ground state. The remaining probability is spread among several levels near 75 keV excitation energy; but these higher excited levels play an insignificant role in capture rates for stellar temperatures near 30 keV, as is illustrated below. The capture correction is thus critically important for the 9.75-keV level, and is made using the statistical model of nuclear reactions to estimate the role of the capture on the $\frac{3}{2}^-$ level through calculation of a factor

$$F = [\langle \sigma_c(186)^* \rangle / \langle \sigma_c(186)L \rangle] \times \langle \sigma_c(187)L \rangle / \langle \sigma_c(187)^* \rangle] . \quad (1)$$

The factor F corrects ground state average capture rates to stellar average capture rates. In Eq. (1) the asterisk denotes stellar average, and L denotes laboratory average. The value of F calculated and used in the Re-Os studies[11,12] is $F=0.83$. But Woosley and Fowler[16] noted that if neutron scattering transmission coefficients (absorption probabilities) for the excited level happened to be much smaller than those for the ground state, then capture from the excited level at stellar temperatures would be weak, the factor F would be >1.1, and the results of the two chronologies would be much closer together.

A consequence of this resolution of the dating inconsistency is that the neutron inelastic scattering cross section to the 9.75-keV level would be quite small—less than 0.3 b for a neutron energy of $\sim$30 keV—since it also depends on absorption probabilities for neutrons incident on the excited level. This suggested resolution, through weak capture from the excited level, and an associated small inelastic scattering cross section [σ(n,n')], was reinforced in one of the Re-Os papers. Winters *et al.*[12] found that a combined analysis of capture rates and neutron and γ-ray strength functions was consistent with a $\sigma(n,n') \sim 0.3$ b for $E_n \sim 30$ keV. The first effort to measure this cross section led to a reported upper limit[17] of $\sigma(n,n') < 0.7$ b at $E_n = 30$ keV. Thus all results seemed to be developing toward consistency, but at the expense of an unusually small inelastic scattering cross section. Such a small value would require severe target-level dependence of scattering probabilities, or scattering amplitudes. Such dependence would depart strongly from the usual analyses, in which a single, neutron energy dependent potential is presumed to be appropriate for all scattering channels.

The experiment and analyses reported here were undertaken to measure the neutron inelastic scattering cross section, and to provide a consistent representation of all observed scattering properties, including the various partial cross sections, for the n+^{187}Os system. A consistent analysis of total, inelastic scattering, and capture cross sections could eliminate the uncertainties[16] associated with the use of different scattering models, and provide confidence that the relationship between the different partial cross sections was understood. The analysis is designed to include also the s- and p-wave strength functions and scattering lengths, where measurements of these properties are available.

The capture cross sections were well measured, the total cross sections[18] and strength functions[17] were being determined just as this experiment began, and some of the other low energy scattering properties were also known. When all of this information is put into an analysis to determine scattering amplitudes, the amplitudes are overdetermined, permitting consistency tests. Transmission coefficients calculated from the scattering amplitudes are actually used to calculate neutron capture and inelastic scattering cross sections, and thus also the stellar correction factor F.

EXPERIMENTAL METHOD

The ^{7}Li(p,n)^{7}Be reaction is the logical one to produce a low energy neutron flux with small energy spread. Berman[19] has suggested this reaction with a proton energy (E_p) very near threshold (E_{th}) as a source of 30 keV neutrons, an ideal energy to match stellar synthesis conditions. But the differential rate of neutron energy change, dE_n/dE_p, is so large just at threshold that $E_p - E_{th} < 0.3$ keV is required to have an adequately small energy spread

incident on the scattering samples. The yield from the source reaction is also quite small within 1 keV of threshold.

An incident energy which gave $E_p - E_{th} = 7$ keV was chosen for this experiment, which would provide $E_n = 62$ keV at 0°. At this energy $dE_n/dE_p = 2.5$, which is still large but much smaller than the slope near threshold. The 0° cross section at that energy is approximately $\frac{2}{3}$ of the maximum cross section above threshold, so the 0° yield is reasonably large. Since the goal in the scattering measurement is to separate a small inelastic group only 9.75 keV from a large elastic one, an effort was made to achieve an overall energy spread of 6—7 keV. The intrinsic spread of the pulsed beam of the accelerator is <0.8 keV, as determined from thick target Li(p,n) yield curves near threshold. Thus the LiF targets used had to be 1.7 keV thick or less to hold the total proton energy spread $\Delta E_p < 2$ keV. To have a target stable for long periods under proton bombardment, and ones which would not have diffused into their backings during vacuum evaporation, LiF was evaporated onto Ni backings 0.1 mm thick. Empirical tests with several backing materials showed that of the materials tested the Ni backings provide the lowest photon backgrounds in our scattered neutron detector.

Time-of-flight (TOF) detection to achieve neutron energy separation together with the availability of isotopically enriched 2 g ^{187}Os and ^{188}Os samples dictated the experimental geometry. The source of the samples and their characteristics, including isotopic abundances, are described in detail in Ref. 12. The physical arrangement of source, sample, and shielded, scattered neutron detector is shown in Fig. 1. The samples are shown as solid disks, one centered in the neutron flux on the proton axis, and the other positioned out of the kinematically limited cone of neutron flux. The edges of the cone are indicated by dashed lines. The two samples were 1 cm diam disks 0.15 cm thick, and had identical masses to within 1 mg. One is enriched to 70% in ^{187}Os and the other to 94.5% in ^{188}Os. These identical size, identical mass enriched samples were very important for the results of this experiment, especially for separating elastic and inelastic scattering yields with confidence.

Two plastic scintillation detectors were used for TOF energy separation, one for detection of scattered neutrons at 90° as shown shielded in Fig. 1, and the other for monitoring incident flux at 0°. The two scintillation detector assemblies are shown in an inset at the lower left in Fig. 1, a small scale isometric overview of the experimental geometry. The scattered neutron detector is the majority-logic system of Hill *et al.*[20] which consists of a plastic scintillator viewed by three photomultipliers. The electronics system[20] of the detector allows a bias low enough to detect neutrons of a few keV with good efficiency, and rather good timing. Tests showed an instrumental resolution of 4 ns for an energy range from 5 to 70 keV. In this experiment, operating at $E_n = 60$ keV, we were interested in detecting 50—60 keV neutrons. The range of pulse heights accepted corresponded to neutrons from 15 to 70 keV, and the detector time resolution was about 3.5 ns.

The detector was housed in a cylindrical Pb shield which itself was surrounded by a 5 cm thick shell of Li_2CO_3 loaded paraffin. A second 1 cm thick Pb case enclosed the assembly. Inside the inner Pb shell a graded shield of Al, Ti, Cu, and Sn was wrapped around the scintillator. The different components of the graded shield had thicknesses of about 100, 150, 100, and 300 μm,

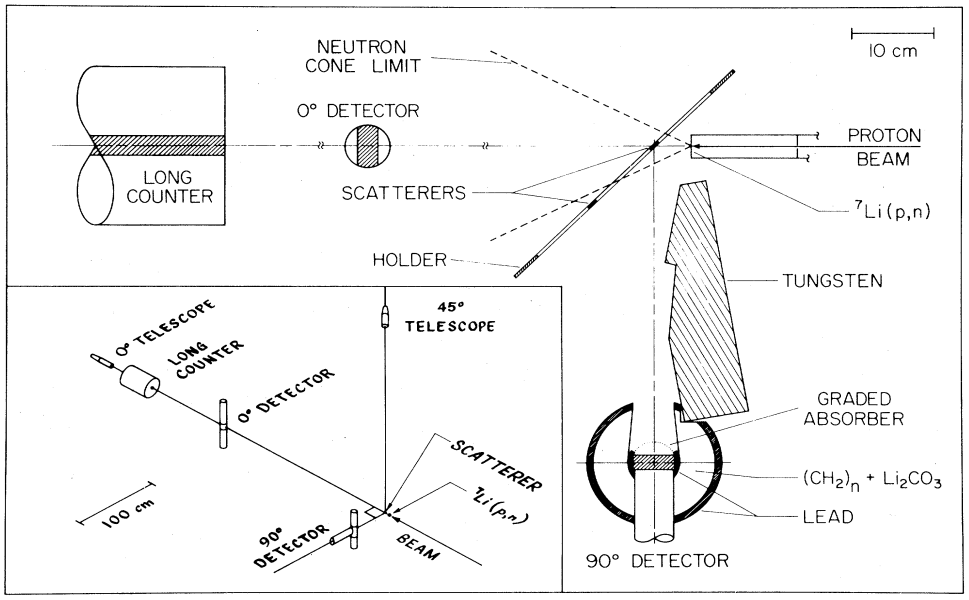

FIG. 1. Scattering geometry showing the shielded 90° detector, the plastic sample holder, and the scatterers. Distances along 0° to the monitors are not shown to scale. The dashed lines show the limiting angles of neutron emission for the incident energy of this experiment. The inset at lower left shows an isometric sketch of the entire system on a small scale.

respectively. This shield was designed to stop soft x rays while being thin enough to transmit neutrons. The shielded detector was mounted to provide a flight path of 40.7 cm from the scattering sample. A large W bar was used to shadow the scintillator and most of its shield from radiation produced at the LiF target. The whole system was the result of much empirical testing of arrangements to minimize backgrounds. The Os samples were mounted by wrapping them in a fold of 0.35×10^{-3} cm Mylar, and the plastic was then heat sealed around the samples. These thin plastic cases were stretched into a large, lightweight plexiglass frame partially shown in Fig. 1. The beam spot on the LiF target was constrained by collimators to within about 1 mm on the target. Had some neutrons been produced outside the cone and thus able to strike the out-of-position sample, the scattered events would have occurred in the TOF spectrum more than 100 ns displaced from the peaks of interest. No such events were observed in the spectrum.

The 0° scintillation detector was a two photomultiplier detector, similar to the 90° detector in size. It was not shielded since, for viewing the 0° flux, background was not a problem. The long counter seen in the inset of Fig. 1 was an additional monitor, and the two telescopes shown were used to position the scattering samples initially. The 45° telescope alone was used for sample repositioning during the sequence of data taking.

The separate instrumental time resolution of the two fast scintillation detectors was about 3—4 ns as operated in this experiment, to provide an energy bias of about 15 keV. When the energy spread implied by this Δt is folded into the ΔE_n of 5 keV from the proton target, the overall energy spread on the sample was expected to be $\Delta E_n \approx 7.5$ keV.

The 0° TOF monitor shown in Fig. 1 was mounted 2.3 m from the neutron source and gave a measured total energy spread of 6.5 keV at an incident energy of 61.3 keV. However the 1 cm diam scattering sample located 4.5 cm from the source subtended an angle large enough ($\pm6.3°$) to broaden the energy spread on the sample to $\Delta E_n \sim 8$ keV; the energy on the samples during data runs was then 60.5 keV. The proton energy was manually adjusted to hold the neutron energy constant to ±0.3 keV, using the 0° monitor to indicate energy. At an incident proton energy of $E_p = E_{th} + 7$ keV the neutron cone opened up to $\pm27.5°$, as shown in Fig. 1. No solid objects other than the scattering samples, their thin plastic suspensions, and the 0° monitors were in the cone. The yields from the long counter, which has an efficiency stable to $\pm0.5\%$, were used to normalize yields from the different sample runs to each other. The neutron energy dependence of the majority-logic detector's efficiency was measured by obtaining no sample runs with thick LiF targets, and with the detector viewing the source at 0°; the proton energy was set to provide a neutron spectrum including neutrons from 5 to 70 keV. Converting the time spectrum from the source into an energy spectrum and dividing the resulting energy dependent yields by the energy dependence of the ^{7}Li(p,n)^{7}Be cross section[18] produced the energy dependent efficiency shown in Fig. 2. The desired property of this curve for this experiment is that between 50 and 60 keV

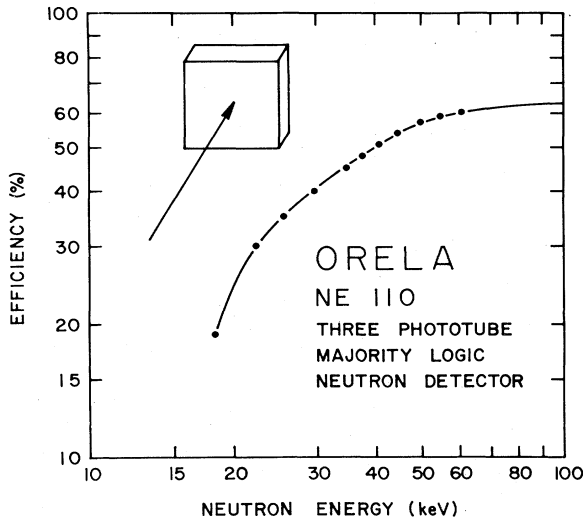

FIG. 2. Measured detection efficiency of the ORELA majority-logic neutron detector, with bias set to accept pulses for neutrons of 15 keV or higher in energy.

the efficiency is large and changes little. The detector size and energy bias were chosen to provide optimum efficiency consistent with the requirement of small scintillator volume, since background is proportional to volume. TOF spectra were taken using thin LiF targets (1.5 keV) and various samples to test background rates and sources. No spurious or instrumental peaks were present, only a time independent background.

Thirty seven data runs were taken alternating the ^{187}Os and ^{188}Os samples, each of approximately 1.5 h duration. The length of the individual runs was set to provide more than 6000 counts in each spectrum. The spectra had a time dispersion of 0.35 ns/channel, and the elastic peaks had half-widths of 27 channels. Runs were individually stored on tape for subsequent comparison and peak-shape analysis. Comparisons of the 18 ^{188}Os spectra and 19 ^{187}Os spectra showed centroid shifts less than one channel from one run to another, consistent with statistics. Each sample's runs were added into sets of three adjacent runs, and the centroids of these sets were compared. Centroid shifts <0.5 channels were found between sets, also consistent with statistics of the summed runs. Following these consistency tests, all of the runs for each sample were added into one composite spectrum. The spectra so obtained are shown in Figs. 3 and 4.

The small inelastic scattering group on the low energy side of the ^{187}Os elastic group is certainly not well resolved, but did visibly distort the peak as is evident in Figs. 3 and 4, and was evident in a direct comparison of every adjacent pair of runs for the two samples.

Small amounts of light element impurities in the Os samples, particularly the ^{187}Os sample, could mimic inelastic scattering at 90°, since the kinematic shift of neutrons scattered from C is 9.4 keV. But chemical analysis of the metal prior to forming it into the compressed, sin-

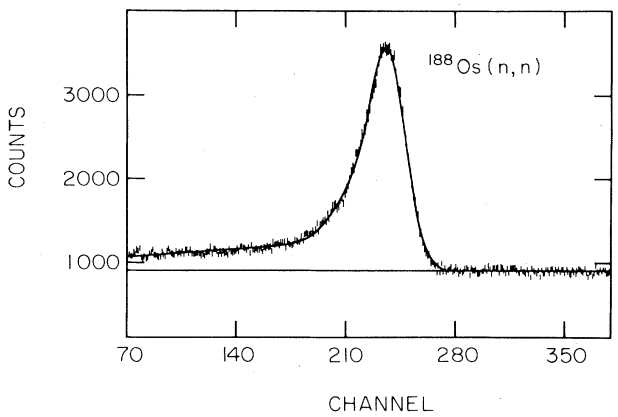

FIG. 3. Neutron elastic scattering spectrum for ^{188}Os. The solid curve through the data is a least squares fit of a double Gaussian peak shape folded with an exponential tail. This fit is shown superimposed upon the flat background observed when no sample was present.

tered samples showed less than 50 ppm oxygen. Moreover the oxides of Os are volatile, and would not survive the heat generated in forming the samples. A test for the presence of C was examination of the scattered neutron spectrum at 135°, where the kinematic shift is 15.1 keV. The peaks observed at that angle had the same shape as the peaks at 90°; the yield of a possible C contaminant could not exceed 20% that of the inelastic component of ^{187}Os, and could not exceed 10% of that yield in the ^{188}Os sample. Test spectra were measured also for small Pb samples, and they showed the same peak shapes as that of Fig. 3.

DATA REDUCTION AND ANALYSIS

Analyzing the shape of the combined groups of Fig. 3 to give the inelastic scattering yield with confidence was greatly aided by the use of these physically identical samples, and the presence of the 0° TOF monitor. The incident neutron flux versus TOF is an asymmetric peak well described by a double Gaussian, with one Gaussian displaced from the other and containing (10—14) % of the peak yield. A symmetric incident energy spread would, on transformation into a TOF scale, become an asymmetric peak; the asymmetry was evident in the 0° monitor. The scattered neutron spectrum at 90° also showed an exponential tail, as is evident in Fig. 3. The tail is associated with neutrons from the scattering sample, and probably arises from sample neutrons multiply scattered in the paraffin-loaded shield surrounding the detector. Such exponential tails are common[1] in neutron spectra for detectors used in large paraffin-loaded collimators. The solid curve shown for ^{188}Os in Fig. 3 is a least squares fit of a compound shape including two Gaussians folded with an exponential tail. This compound shape is superimposed upon a time independent background, which is what is observed when no sample is present. This fit determined the shape of a peak for a single group, and gave a reduced χ^2 of 1.25. With the shape parameters thus fixed, a fit to the combined elastic plus inelastic data of the ^{187}Os sample was made. This fit used only four independent parameters: (1) the uniform background level, (2) the amplitude for elastic scattering, (3) the amplitude for inelastic scattering, and (4) the position of the elastic scattering peak. The curves of Fig. 4 are the fits. The solid curve is the combined fit to all of the data, and the dashed curve is the elastic peak only. In a lower panel of the figure is shown the difference between the data and the elastic fit, together with a curve produced with the parameters for the inelastic scattering group. Throughout the fitting the centroids and half-height points of the elastic and inelastic components were constrained to be separated by the known excitation energy, 9.75 keV. The reduced χ^2 for the composite ^{187}Os peak is 1.3, in good accord with the value obtained in fitting ^{188}Os.

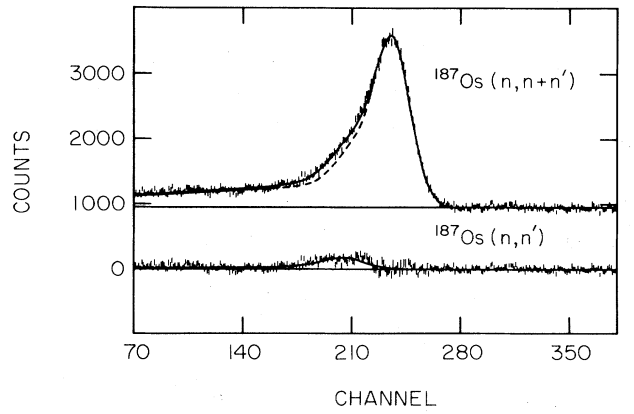

FIG. 4. Composite scattering spectrum for ^{187}Os. The upper solid curve shows the fit to both the elastic and inelastic components. The dashed curve shows the elastic curve alone, with shape parameters taken from the fit of Fig. 3. The lower panel shows the data obtained by subtracting the dashed curve from the data, and the solid curve is the part of the composite fit which comes from the parameters of the inelastic scattering group.

Earlier three parameter attempts to fit the ^{187}Os data also constrained the centroid of the elastic group to be the same as that for ^{188}Os. But the resulting fits had considerably worse reduced χ^2 than those of Fig. 4, and the calculation was clearly shifted with respect to the data. Thus it was determined that the elastic group of one sample was shifted with respect to the other by 0.9 channels, or ~0.3 ns. The only source of a consistent shift between the two samples, with samples being interchanged and repositioned some 40 times during a five day running period, was a fixed physical displacement between the two samples normal to the plastic mounting frame of Fig. 1. The telescope arrangement used in Fig. 1 would not have been very good for detecting such a displacement. Subsequent examination of the plastic frame and Mylar film mountings indicated that a displacement of ~0.5 mm would have been possible, and the 0.9 channel shift between sample time peaks would correspond to a displacement of ~0.7 mm. These details are mentioned to show the sensitivity with which the peak parameters are determined by the data.

The result of the Fig. 4 fit is that the ratio R of inelastic to elastic yield is (7.5±0.5) %. After this ratio was deter-

mined for the ^{187}Os data the ^{188}Os spectrum was refitted, attempting to include an inelastic component. From the resulting fit, the ratio R_8 was determined to be $R_8=(-0.004\pm0.4)\%$, consistent with the negligible abundance (0.17%) of ^{187}Os in the ^{188}Os sample. The fitting procedure which gives us the yield of inelastic scattering in ^{187}Os also correctly provides no inelastic scattering for the ^{188}Os sample.

Additional scattering data were taken to measure the angular dependence of yields for scattering angles of 45°, 90°, and 135°. The purpose of these angular asymmetry measurements was to help constrain the relationship between s- and p-wave scattering amplitudes. In these data the elastic and inelastic ^{187}Os components were not separated; only the yields of the combined groups were obtained. The yields were described as

$$W(\theta)=A[1+a_1\cos(\theta)]\ ,$$

$$a_1=0.13\pm0.02$$

for the ^{188}Os sample. Using the ratio R for ^{187}Os, and noting that the inelastic scattering is isotropic, yields an asymmetry $a_1=0.12$ for the elastic component of the ^{187}Os sample. In principle there should be a $\cos^2(\theta)$ term also, but it would be $\propto(a_1)^2$, and too small to fix in this experiment.

High precision total cross section (σ_t) measurements have recently been completed at ORELA from the resonance region up to about 100 keV.[18] These data together with the accurately known[11,12] capture cross sections (σ_c) provide us with another consistency check on our 90° scattering data. Averaging the σ_t values over 10 keV to approximate our conditions, and subtracting similar averages of capture cross sections, we obtain the following scattering cross sections at 60 keV:

$$\sigma_{sc}=\langle\sigma_t(188)\rangle-\langle\sigma_c(188)\rangle=12.0\text{ b}$$

and

$$\sigma_{sc}=\langle\sigma_t(187)\rangle-\langle\sigma_c(187)\rangle=12.1\text{ b}\ .$$

Because $W(\theta)$ for elastic scattering has a simple $\cos(\theta)$ dependence, 90° yields sample angle integrated cross sections. Thus the σ_{sc} given above, together with isotopic abundances of these two enriched samples, can be used to estimate the ratio of scattering yields for the two samples. The estimate is uncertain at the 2–3% level, because cross sections for other isotopes are not available. We find, using the σ_{sc} values above, that at 90° $Y(188)/Y(187)$ should be 0.99. The measured yields at 90° provide the ratio 1.00 ± 0.01, which is good agreement.

Our scattering yields are then converted to cross sections by normalization to the σ_{sc} values, and the percentage of inelastic scattering provides the inelastic scattering cross section, $\sigma(n,n')$.

The conversion of inelastic scattering yields to a cross section requires corrections for the energy dependence of neutron detection efficiency, shown in Fig. 2 (3.3%), for multiple elastic and multiple inelastic scattering in the sample (12%), and for the ^{187}Os abundance (70.4%). With these corrections, the result at $E_n=60$ keV with a spread $\Delta E_n=8$ keV is

$$\sigma(n,n')=1.13\pm0.2\text{ b}\ .$$

The elastic scattering cross section for ^{187}Os is then $\sigma_e=11.0$ b.

ANALYSIS AND INTERPRETATION

The goal of the analyses reported here is to obtain a consistent description of all of the low energy neutron scattering properties, to provide confidence that the ^{187}Os+n system is well characterized. Properties included in the analyses are the s- and p-wave strength functions (s_0 and s_1), the scattering lengths R', the total cross sections of Ref. 18, the capture cross sections of Refs. 11 and 12, and the scattering cross sections of this experiment. Analyses are concluded for both ^{187}Os and ^{188}Os using two independent methods; consistent results from both methods strengthens confidence in the conclusions.

The first analysis method relies on a direct description of the total cross sections, elastic scattering anisotropies, and s- and p-wave strength functions in terms of energy averaged scattering amplitudes. Transmission coefficients obtained from the amplitudes are then used in the statistical model to calculate partial cross sections. Both the inelastic scattering and capture cross sections are computed for comparison with the measurements. The advantage of this method is that the determination of the scattering amplitudes and the transmission coefficients can be model independent. Calculation of the (n,n') and (n,γ) cross sections does depend on the validity of the statistical model, a subject to be discussed in detail later. Many experiments and analyses have shown that in the absence of polarizations low energy scattering is quite insensitive to spin-orbit interactions. Thus spin dependence is ignored in the scattering amplitudes.

In terms of energy averaged scattering amplitudes the differential cross section for elastic scattering may be written

$$d\sigma/d\omega=\pi\lambda\!\!\!^{-2}\sum_l[(2l+1)^{1/2}(1-\langle\eta_l\rangle)Y_l^0]^2 \qquad (2)$$

with l as the orbital angular momentum, $\langle\eta_l\rangle$ the complex scattering amplitude, and Y_l^0 the lth order spherical harmonic. The transmission coefficients needed, T_l, are determined from the scattering amplitudes:

$$T_l=1-|\langle\eta_l\rangle|^2\ . \qquad (3)$$

The total cross section is also simply written in terms of the scattering amplitudes:

$$\sigma_t=2\pi\lambda\!\!\!^{-2}\sum_l(2l+1)(1-\mathrm{Re}\{\langle\eta_l\rangle\})\ . \qquad (4)$$

Using the extracted coefficients, T_l, and the statistical model, one writes, for the various partial cross sections,

$$\sigma(n,\alpha)=\frac{\pi\lambda\!\!\!^{-2}}{2(2I+1)}\sum_J\left[(2J+1)T_l^nT_l^\alpha\Big/\sum_\delta{}'T_\delta\right]\ . \qquad (5)$$

The primed sum indicates a sum over all open channels belonging to the angular momentum of the compound system, J. The target nucleus has ground state spin I. Even though it is not necessary to consider spin dependence in

calculating the scattering amplitudes and transmission coefficients, the J dependence of the partial cross sections must be correctly stated, to count the statistical weights and scattering probabilities of different channels correctly.

The procedure followed was to vary the $\mathrm{Re}\{\langle\eta_l\rangle\}$ and the $\mathrm{Im}\{\langle\eta_l\rangle\}$ to provide a fit to total cross sections and the scattering anisotropy coefficients a_1. At these low energies only s and p waves contributed significantly, so only four parameters needed to be varied. The resulting T_l values together with the γ-ray transmission coefficients of Ref. 11 were then used in the usual statistical model to calculate the $\sigma(\mathrm{n,n'})$ and $\sigma(\mathrm{n},\gamma)$.

In the course of the fitting, total cross sections, elastic and inelastic scattering cross sections, and capture cross sections were all calculated. The published values for s- and p-wave strength functions for natural Os were the starting point of the analysis. From these, extrapolated to the 60 keV incident energy of the experiment, starting values for the $|\langle\eta_l\rangle|$ were obtained. The starting phases of $\langle\eta_l\rangle$ were chosen as those of a realistic neutron scattering potential. From this approach it was clear that the then known s_0 for natural Os could not be made consistent with the total cross sections and elastic scattering anisotropies. The fitting procedure also resulted in both capture and (n,n') cross sections well below the values of Refs. 11 and 12, and of this experiment. Following this failure, the procedure was changed to include some consideration of the capture and inelastic scattering cross sections in the analysis, and exclude the s-wave strength function. Now the scattering amplitudes fitted did depend to some extent on the statistical model. In the new approach scattering amplitudes were determined which fit the elastic scattering anisotropies, and total and nonelastic cross sections; the last is just the sum of the (n,n') and capture cross sections. In the course of that fit, we found that a value of $s_0 = 3.4 \times 10^{-4}$ resulted from the scattering amplitudes found. The results of the entire parametrization are given in Table I. After that fit had been concluded, a new measurement of strength functions was reported,[17] which provided the measured values given in Table I. The unexpectedly large s_0 and even a 20% reduction of the value of Ref. 11 for s_1 were subsequently verified by the new measurements of Ref. 17.

The report of new results for strength functions of ^{187}Os, to which we had been independently driven in our cross sections analysis, encouraged us to reexamine our fitting procedure, and ascertain that those together with the total cross sections and elastic scattering anisotropies were sufficient to constrain the four scattering amplitudes, real and imaginary parts for s and p waves. With the new strength functions of Winters *et al.*[17] we have a representation of all known scattering properties, including capture cross sections and scattering cross sections of this experiment, which is entirely consistent.

The second method of analysis chosen was that of standard spherical potential models. In that method the number of partial waves contributing was not artificially restricted, and spin-orbit dependence in the potential was included. Once again, the starting points of the analysis were the recently measured[18] total cross sections for the two Os isotopes, and the newly reported strength functions for ^{187}Os. These constrained the parameters of a scattering potential, from which transmission coefficients were obtained. The statistical model was then used with these coefficients and the γ-ray strength functions of Ref. 11, as updated in Ref. 17, to calculate inelastic scattering and capture cross sections. A slightly different γ-ray strength function was used for one calculation of capture in ^{187}Os, as noted below.

The results of the two analysis methods, one with and one without employing a neutron scattering potential, are shown in Table I. Shown also are the measurements from this and other experiments. As is evident, a better fit to most observables is possible when the scattering amplitudes are not constrained to be those of a potential; but both analyses provide good representations of the n+^{187}Os- system. As noted, in the first or amplitude-fitting analysis the γ-ray strength function needed to fit

TABLE I. Measured and calculated scattering properties for ^{187,188}Os at 60 keV neutron energy. Method 1 refers to calculations from fits of scattering amplitudes to scattering observables. Method 2 refers to analysis with a scattering potential. σ_t and $\sigma(\mathrm{n,n'})$ denote total and inelastic scattering cross sections, respectively. σ_c denotes the capture cross section, a_1 denotes elastic scattering anisotropy, and s_0 and s_1 denote strength functions. All cross sections are expressed in mb.

	σ_t	$\sigma(\mathrm{n,n'})$	σ_c	a_1	s_0 ($\times 10^4$)	s_1
^{187}Os						
Measured	12.75	1.13	0.60	0.11	3.5	0.35
Calculated						
Method 1	12.7	1.35	0.62	0.11	3.4	0.40
Method 2	12.6	1.44	0.78		2.8	0.90
^{188}Os						
Measured	12.3		0.30	0.13	2.2	
Calculated						
Method 1	12.25		0.29	0.13	2.2	
Method 2	12.6		0.30		2.3	

the capture cross sections was independently determined here to be just that reported in Ref. 17. For the capture calculations of method 2 it was necessary to reduce the γ-ray strength 25% below that recently suggested[17] for ^{187}Os.

The incident neutron energy dependencies of the inelastic scattering and capture cross sections are needed for average capture rate calculations and are readily obtained from analyses using scattering codes and potentials; such energy dependence is shown for potential models in Fig. 5, for σ(n,n'). The highest and lowest curves are from the potential parametrization used for the results called "method 2" in Table I. This potential leads to a low value for the s wave strength function, but one within the limits allowed by the quoted errors[17] of measurements. All partial cross sections were calculated in the Wolfenstein-Hauser-Feshbach (WHF) model for the upper (dashed) curve; the inelastic scattering cross sections are high compared to the measurements, reflecting the need for a modified form of the statistical model[1] incorporating width fluctuation and channel-channel correlation corrections.[21]

The lowest (dotted-dashed) curve is calculated using the same potential as for the dashed curve, but now Lane-Dresner level-width fluctuation corrections[21] are included; these substantially reduce inelastic scattering cross sections when only two strongly excited levels are in the model space, as is the case here. A more realistic model would be one in which channel-channel correlation corrections are also included. It is now well known[21] that applying only level-width fluctuation corrections seriously underestimates inelastic scattering cross sections, since channel-channel correlations enhance σ(n,n') enough to cancel most of the level-width fluctuation corrections. This near cancellation exists when there are strong correlations between partial width amplitudes in different channels. That such correlations exist and are often large has been directly demonstrated in recent resonance experiments with protons.[22] An approximate procedure for including correlation corrections has been given by Tepel *et al.*[23] and has been used here to estimate the effects of both width fluctuation and correlation corrections. The results of that model provide a calculated curve which runs 20% below the WHF calculation, or dashed curve, in Fig. 5.

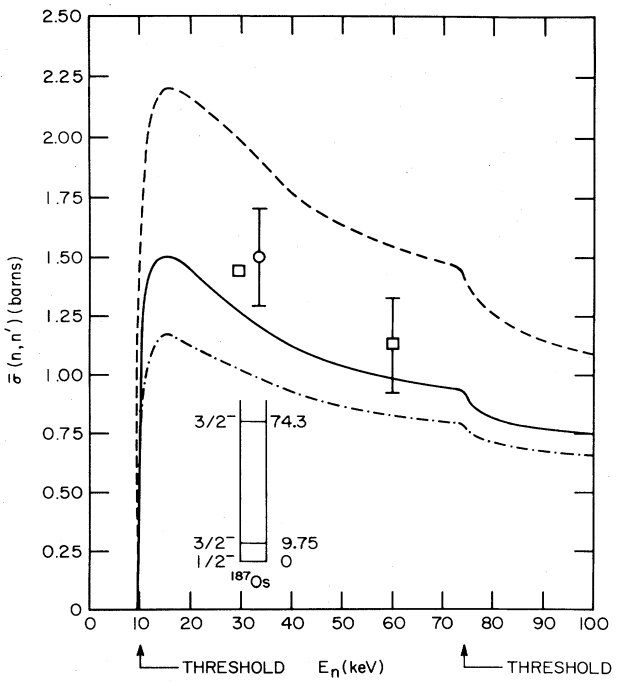

FIG. 5. Measured and calculated inelastic scattering cross sections for scattering to the 9.75-keV level. The square point at 60 keV is the measurement of this experiment, and the square at 30 keV is extrapolated from 60 keV using the energy dependence of the calculations. The circular point at 34 keV is the ORELA measurement mentioned in the text. The dashed and dotted-dashed curves show the extremes allowed by the unmodified WHF model and the Lane-Dresner corrections. The two solid curves show realistic assessments of the lower and upper limits allowed by realistic statistical models.

The solid curve of Fig. 5 comes from calculations with a quite different model. The potential parameters were fixed to reproduce precisely the newly reported $s_0 = 3.5 \times 10^{-4}$ and the total cross sections. The transmission coefficients from that potential were used in a statistical model which incorporates only the Lane-Dresner level-width fluctuation corrections.[21] Thus we must expect that the solid curve of Fig. 5 is a lower limit to partial cross sections with the potential which fits strength functions and total cross sections well, and 20% below the upper or dashed curve is an upper limit for the inelastic scattering calculations. The break in the calculated curves near 74 keV results from crossing thresholds for higher excited levels. The size of that break shows that the higher levels have a very small effect on reaction rates for stellar temperatures near 10—50 keV.

The points shown in Fig. 5 are measurements, and an extrapolation of a measurement. The value plotted at 60.5 keV is our measured value, and it is extrapolated to 30 keV using the energy dependence of the calculations shown in Fig. 5. The value shown for 34 keV is a result of Macklin *et al.*[24] who measured the inelastic scattering cross section with a very different method than that used here. The agreement between the extrapolated and measured values near 30 keV is very encouraging.

The γ-ray strengths, or capture γ-ray widths, used in this second potential model have the usual J dependence[14] associated with capture widths, instead of a constant strength for all capture channels as was used for the results in Table I, and in Refs. 11 and 17. However, from the J-dependent capture widths used in the second potential model one can construct a J-weighted average γ-ray strength function. When this is done, the average strength is just that quoted in Ref. 17, or 20% reduced from the value used in Ref. 11.

These calculations are really needed not to fit precisely the inelastic scattering cross sections, but to provide realistic means of extrapolating the cross sections from our measurement energy of 60 keV throughout the astrophysically interesting energy region. For that purpose it is en-

couraging to note that the two potential models of Fig. 5, and all three calculations, have the same energy dependence. It is, of course, the capture cross sections which we are most interested in calculating and following as a function of energy, in order to fix the correction factor F discussed in the Introduction. Measured capture cross sections are very well fit, within experimental uncertainties,[11,12] with the model which gives the solid curve of Fig. 5. For example the measured capture cross section for ^{187}Os in Table I can be extrapolated to 30 keV. The result is $\sigma(n,\gamma)=0.95$ b, which is in excellent agreement with measurements of Refs. 11 and 12; they report $\sigma(n,\gamma)=0.87$ and 0.89 b, respectively. Interestingly, also, the level-width fluctuation corrections which have such drastic effects on inelastic scattering cross sections reduce capture cross sections only 10%.

It is worth noting that the two additional assumptions of the first analysis procedure were nicely confirmed in the potential analyses—the spin dependence of the scattering amplitudes is negligible, and partial waves beyond p waves are negligible.

The good agreement between measured observables and those calculated from these analyses (Table I and the solid curve of Fig. 5) means that scattering amplitudes have been successfully adjusted to represent cross sections, including the capture cross sections. The general consistency between the two methods reinforces our confidence in the validity of the characterization of the n + Os system. This is very important to our having confidence in the model calculations of capture cross sections from the 9.75-keV excited level of ^{187} Os, a process important in stars but not measurable in the laboratory.

The third and final step in the analyses is to assess the importance of direct inelastic scattering through deformation induced channel coupling. For coupled-channels calculations we used the code ECIS-79 of Raynal[25] with a simple rotational model form factor. This calculation provides a direct reaction contribution of <10 mb, less than 1% of measured cross sections. This small direct component is not so surprising when one realizes that below 70 keV inelastic scattering is almost entirely s wave, and quadrupole coupling mixes different partial waves.

The Maxwellian averaged capture cross sections for a temperature of 30 keV had been calculated with the statistical model, and with transmission coefficients from various scattering models.[16] Through these calculations tables were prepared presenting the correction factor F for different combinations of possible capture and inelastic scattering cross sections. From a comparison of our results with these previously calculated tables,[16] $F=0.82$ is indicated. It is also clear from direct calculations with our potentials that for any reasonable variation of parameters, F is insensitive to such variations, varying only from 0.80 to 0.83. Thus F seems to be rather well fixed, now that the possibility of anomalously low inelastic scattering cross sections has been eliminated. With this correction factor, the duration of nucleosynthesis as determined in the Re-Os chronology becomes $\Delta > 12.5$ Gyr, as noted in the Introduction. In a recent communication Woosley and Fowler have reanalyzed cross sections in the light of the new measurements reported here,[26] and find the value $F=0.80$.

This experiment and analyses were begun and executed when a short period of nucleosynthesis, $\Delta=6.1\pm2.3$ Gyr, seemed firmly indicated from the reexamination of the U-Th chronology by Fowler,[5] as described in the Introduction. Now, after showing conclusively that n+Os scattering is at least largely in accord with conventional potentials, the possibility that the scattering cross sections would permit a large decrease in the ages implied by Re-Os chronology is eliminated. The period of nucleosynthesis from that chronology is twice the value given above in 1978 for the U-Th results.

The estimate of galactic age given from the Re-Os chronology is subject to some uncertainty associated with modifications of the decay rate of ^{187}Re resident in stellar interiors. In large stars this modification can be quite large,[27] but the time in such stars should be small compared to the galactic age. Nonetheless, this possible modification contributes about $\pm20\%$ uncertainty to the galactic age.[27] An important uncertainty is associated also with the presumed r-process history, for all r-process dependent chronologies.

Just as this manuscript was being prepared, results[28] were made available from Thielmann, Metzinger, and Klapdor which drastically altered the time scale of the U-Th chronology. By careful consideration of β-delayed fission probabilities, making use of rather new information about Gamov-Teller strength distributions in nuclei and recently available fission barrier heights,[28] they were able to show that fission plays a much greater role in nuclear decay near the Th and U nuclei than previously expected. Making carefully detailed calculations of fission and neutron emission probabilities from nuclei formed through the r process, they showed that the U-Th chronology leads to a galactic age of 20.8^{+2}_{-4} Gyr or a period of nucleosynthesis of $\Delta=16^{+2}_{-4}$ Gyr, consistent with the results cited in the Introduction, and confirmed in this study, for the Re-Os chronology. Thus, once again the two nucleochronologies are reconciled but now at a much larger age than expected in 1978.

SUMMARY

Careful measurements of neutron elastic and inelastic scattering from ^{188}Os and ^{187}Os provide cross sections well represented, together with previously measured capture cross sections and other neutron scattering observables, in a standard scattering amplitude codification. Using these scattering amplitudes and the statistical model describes well the $\sigma(n,n')=1.13$ b measured at 60.5 keV, and projects a cross section of 1.45 b at 30 keV. This agreement could only be obtained by requiring an s-wave strength function of $\sim3.4\times10^{-4}$. This result was later seen to be in good agreement with the reevaluated s_0 of Carlton and Winters, from neutron resonance cross sections. These results and calculations of the stellar capture correction factor of Woolsey and Fowler confirmed the earlier result of $\Delta > 12.5$ Gyr for nucleosynthesis duration. With the reexamination of the U-Th chronology just now being concluded, both chronologies of concern in this paper lead to galactic ages in agreement.

ACKNOWLEDGMENTS

The authors wish to acknowledge especially the encouragement and support of J. A. Harvey, who made use of the isotopically enriched Os samples in the Kentucky laboratory a simple matter, and who expedited use of the ORNL majority-logic detector. We are also indebted to R. Carlton of Middle Tennessee Technological University and R. Winters of Denison University, who kindly provided total cross section measurements for the Os isotopes prior to publication. The analyses of this paper would have been less definitive without those measurements. We appreciate also the assistance of Mr. Z. Cao with potential determinations. The Denison University workshop on the Re-Os chronology and other problems of nuclear astrophysics in 1982 provided us with opportunities for valuable consultations with Professor Winters and with Professor W. A. Fowler of Caltech. We appreciate also a communication from F.-K. Thielemann of Munich of his forthcoming study of the synthesis of heavy elements, and the U-Th chronology. This work was partially supported under National Science Foundation Grant No. PHY81-05525 and by the Department of Energy Contract No. W-7405-ENG-26 operated by the Union Carbide Corporation.

---

*Permanent address: Engineering Physics Division, ORELA, Oak Ridge National Laboratory, Oak Ridge, TN 37830.

[1]D. F. Coope, S. N. Tripathi, M. C. Schell, J. L. Weil, and M. T. McEllistrem, Phys. Rev. C 16, 2223 (1977); J. P. Delaroche, G. Haouat, J. Lachkar, Y. Patin, J. Sigaud, and J. Chardine, *ibid.* 23, 136 (1981); D. W. S. Chan, J. J. Egan, A. Mittler, and E. Sheldon, *ibid.* 26, 841 (1982).

[2]D. D. Clayton, *Principles of Stellar Evolution and Nucleosynthesis* (McGraw-Hill, New York, 1968); B. A. Allen, J. H. Gibbons, and R. L. Macklin, in *Advances in Nuclear Physics 4,* edited by E. Vogt (Plenum, New York, 1971), p. 255; J. Browne and B. Berman, Nature 262, 197 (1976).

[3]R. G. Ostic, R. D. Russell, and P. H. Reynolds, Nature 199, 1160 (1963).

[4]W. A. Fowler and F. Hoyle, Ann. Phys. (N.Y.) 10, 280 (1960).

[5]W. A. Fowler, in *Proceedings of the Robert A. Welch Foundation on Cosmochemistry,* edited by W. O. Milligan (Welch Foundation, Houston, Texas, 1978).

[6]Bruce A. Twarog, Astrophys. J. 242, 242 (1980).

[7]Beatrice M. Tinsley, Astrophys. J. 250, 758 (1981).

[8]D. D. Clayton, Astrophys. J. 139, 637 (1964).

[9]W. Herr, W. Hoffmeister, B. Hirt, J. Geiss, and F. G. Houtermans, Z. Naturforsch. 16a, 1053 (1961); B. Hirt, G. R. Tilton, W. Herr, and W. Hoffmeister, in *Earth Science and Meteorites,* edited by J. Geiss and E. E. Goldberg (North-Holland, Amsterdam, 1963); R. L. Brodzinski and D. C. Conway, Phys. Rev. 138, B1368 (1965); J. M. Luck, J. L. Birck, and C. T. Allegre, Nature 283, 256 (1980); J. M. Luck and C. T. Allegre, *ibid.* 302, 130 (1983).

[10]R. L. Macklin, J. H. Gibbons, and T. Inada, Nature 197, 369 (1963); R. L. Macklin, T. Inada, and J. H. Gibbons, *ibid.* 194, 1272 (1962).

[11]J. C. Browne and B. L. Berman, Phys. Rev. C 23, 1434 (1981), and earlier work cited therein.

[12]R. R. Winters, R. L. Macklin, and J. Halperin, Phys. Rev. C 21, 563 (1980).

[13]W. A. Fowler, in *Cosmology, Fusion, and Other Matters,* edited by F. Reines (Colorado State University Press, Fort Collins, 1972).

[14]W. A. Fowler, in the Proceeedings of the Workshop on Re-Os Cosmochronology, Denison University, Granville, Ohio, (1982); private communication.

[15]W. A. Fowler, Bull. Am. Astron. Soc. 4, 412 (1972).

[16]S. E. Woosley and William A. Fowler, Astrophys. J. 233, 411 (1979); private communication to R. R. Winters.

[17]R. R. Winters, R. F. Carlton, J. A. Harvey, and N. W. Hill, in the Proceedings of the International Conference on Nuclear Data for Science and Technology, Antwerp, Belgium, 1982.

[18]R. R. Winters, R. F. Carlton, N. W. Hill, and J. A. Harvey, in the Proceedings of the Conference on the 50th Anniversary of the Neutron and its Applications, Cambridge, England, 1982; submitted to Phys. Rev. C.

[19]R. R. Winters, F. Kappeler, K. Wisshak, B. L. Berman, and J. C. Browne, Bull. Am. Phys. Soc. 24, 854 (1979).

[20]N. W. Hill, J. A. Harvey, D. J. Horen, G. L. Morgan, and R. R. Winters, submitted to Nucl. Instrum. Methods.

[21]P. A. Moldauer, Phys. Rev. C 11, 426 (1975); 12, 744 (1975).

[22]W. K. Wells, E. G. Bilpuch, and G. E. Mitchell, Z. Phys. A 297, 215 (1980); W. A. Watson III, E. G. Bilpuch, and G. E. Mitchell, *ibid.* 300, 89 (1981).

[23]J. W. Tepel, H. M. Hofmann, and H. A. Weidenmuller, Phys. Lett. 49B, 1 (1974).

[24]R. L. Macklin, R. R. Winters, and N. W. Hill, submitted to Astrophys. J.

[25]J. Raynal, Saclay Report No. IAEA-SMR-918, 1972; J. Raynal, in *Computing as a Language of Physics* (Trieste, Italy, 1971); M. A. Melkanoff, J. Raynal, and T. Sawada, Math. Comput. Phys. 6, 2 (1966).

[26]W. A. Fowler, private communication.

[27]K. Yokoi, K. Takahashi, and M. Arnould, Astron. Astrophys. 117, 65 (1983).

[28]F.-K. Thielemann, J. Metzinger, and H. V. Klapdor, Z. Phys. A 309, 301 (1983); submitted to Astron. Astrophys.